NASA Contractor Report 145277

COMPUTATION OF THEORETICAL BRIGHTNESS TEMPERATURE CORRESPONDING TO THE CAPE CODE CANAL RADIOMETER MEASUREMENTS

(NASA-CR-145277) COMPUTATION OF THEORETICAL BRIGHTNESS TEMPERATURES CORRESPONDING TO THE CAPE COD CANAL RADIOMETER MEASUREMENTS Final Report (Wentz (Frank J.) and Associates) 14 p HC A02/MF A01 CSCL 08J G3/48

N78-13716

Unclas 55177

FRANK J. WENTZ

FRANK J. WENTZ AND ASSOCIATES
BOX 162, MIT BRANCH P. O.
CAMBRIDGE, MA 02139

NASA PURCHASE ORDER L-24420A

NASA
National Aeronautics and
Space Administration

Langley Research Center
Hampton, Virginia 23665

TABLE OF CONTENTS

COMPUTATION OF THEORETICAL BRIGHTNESS TEMPERATURES CORRESPONDING TO THE CAPE COD CANAL RADIOMETER MEASUREMENTS

Introduction

The potential of microwave radiometers on earth satellites to sense the sea-surface temperature and roughness on an all-weather basis has generated interest in theoretical models for sea brightness temperatures (T_B). Wentz [1975] computed T_B from a two-scale scattering model and compared the results with Hollinger's [1971] radiometer measurements. Although the overall agreement was good, discrepancies did exist and were probably due in part to errors in specifying the input parameters for the T_B model. Also an incomplete correction for the antenna patterns could have contributed to the disagreements.

The extensive ground-truth data collected in conjunction with recent radiometer measurements of the Cape Cod Canal [Swift, 1974] and the improved determination of the permittivity of saline water [C. T. Swift, private communication, 1975] now allow for a more accurate specification of the T_B model's input parameters. In addition, Beck [1975] has computed the corrections to T_B resulting from the Cape Cod Canal radiometer antenna patterns. In this report these investigations are used to take a closer look at the T_B model. First the input parameters are determined from the ground-truth data, and then the computations are compared with the radiometer measurements.

Input Parameters

The T_B model developed by Wentz [1975] requires the following inputs.

Operational Parameters

1. Radiometer frequency f
2. Radiometer polarization P
3. Radiometer viewing angle θ

Environmental Parameters

1. Water surface temperature T_w
2. Water salinity s
3. Power spectrum $S(\kappa)$ of the water surface, κ = wavenumber
4. Downward sky T_B angular distribution $T_s(\theta_z)$, θ_z = zenith angle

The operational parameters for the Cape Cod Canal measurements are f = 1.4, 4.0, and 7.5 GHz; P = horizontal and vertical; and θ ranging from 20° to 70°. Computations are done at the three frequencies, two polarizations, and for θ from 0° to 70° in 10° steps.

Two environmental cases are considered: one between the hours of 1840 and 1852 EDT on May 25, 1972, during which the canal's surface was rough, and the other between the hours of 0126 and 0138 EDT on May 26, 1972, during which the canal's surface was smooth. The ground-truth data required by the model are given in Table 1 for each case.

Table 1. Ground-Truth Data

	Rough Surface	Smooth Surface
Water Temperature	286.1°K	283.9°K
Water Salinity	28 °/oo	28 °/oo
Air Temperature[1]	282.6°K	279.8°K
Wind Speed[1]	14 m/s	6 m/s

[1]Measured approximately 58 m above the canal surface

Permittivity of the Canal Water

The permittivity ε of saline water is a function of the water temperature T_w, salinity s, and frequency f. Swift's [private communication, 1975] expressions for $\varepsilon(T_w,s,f)$, which are based in part on the waveguide measurements of Ho and Hall [1973], are used, and the results are given in Table 2.

Table 2. Permittivity of Canal Water

Frequency	Rough Surface	Smooth Surface
1.4 GHz	75.40 - 50.37j	75.91 - 48.02j
4.0 GHz	70.09 - 33.94j	69.91 - 34.41j
7.5 GHz	59.56 - 36.87j	58.34 - 37.73j

Power Spectrum of the Canal Surface

The smooth surface was described as slick, and the wavestaff record was virtually level. In view of this, a specular surface is assumed for the smooth-surface computations. The rough-surface computations require that the surface power spectrum be specified. Information about the directional properties of the power spectrum of a wind-driven water surface is scarce, especially for a canal with an appreciable current, and the simplifying assumption that the spectrum is isotropic is made. Although the assumption is unrealistic, the anisotrophies will probably tend to average out because the T_B computations involve integrations over all scatter directions.

The isotropic power spectrum $S(\kappa)$ for $\kappa \leq 10^{-3}$ cm^{-1} was measured by a lasar profilometer and by a wavestaff. However, this spectral region is unimportant to the T_B model because it contributes negligibly to the surface slope variance. The important part of the spectrum is $\kappa > 10^{-3}$ cm^{-1} for which no ground-truth spectral data is available. In order to specify $S(\kappa)$ in this region, the friction velocity u_* corresponding to a 14 m/s wind in a neutral atmosphere at 58 m above the surface is calculated from expressions given by Cardone [1969]. The result, u_* = 51 cm/s, is then inputted into Pierson and Stacy's [1973] expressions for the power spectrum of capillary waves (Eqs. 2.7, 2.8, and 2.9 in their report). In this way $S(\kappa)$ is determined for $\kappa \geq 0.359$ cm^{-1}. One should note that Cardone's expressions are for an open sea and the Pierson-Stacy expressions are based on wave tank measurements. Applying these expressions to a canal possibly introduces significant error.

The capillary power spectrum is connected to the ground-truth power spectrum by drawing a straight line on a log $S(\kappa)$ versus log κ plot. This results in the following expressions:

$$S(\kappa) = S(\kappa_1)\,(\kappa_1/\kappa)^d \quad \text{for} \quad \kappa_1 < \kappa < \kappa_2 \tag{1}$$

$$d = \log[S(\kappa_1)/S(\kappa_2)]/\log(\kappa_2/\kappa_1) \tag{2}$$

$$\kappa_1 = 10^{-3}\ \text{cm}^{-1} \tag{3}$$

$$\kappa_2 = 0.359\ \text{cm}^{-1} \tag{4}$$

$$S(\kappa_1) = 1.2\times10^3\ \text{cm}^3 \quad \text{(laser profilometer)} \tag{5}$$

$$S(\kappa_2) = 0.372\ \text{cm}^3 \quad \text{(Pierson-Stacy)} \tag{6}$$

The spectrum for $\kappa < 10^{-3}$ cm^{-1} can be empirically found from the laser profilometer data, but this is not necessary because inspection shows that this portion of the spectrum contributes less than 10^{-5} to the slope variance.

The treatment of two-scale scattering requires that $S(\kappa)$ be divided into a large-scale spectrum $S_\ell(\kappa)$ and a small-scale spectrum $S_s(\kappa)$.

$$S_\ell(\kappa) = \begin{cases} S(\kappa) & \kappa \le \kappa_c \\ 0 & \kappa > \kappa_c \end{cases} \tag{7}$$

$$S_s(\kappa) = \begin{cases} 0 & \kappa \le \kappa_c \\ S(\kappa) & \kappa > \kappa_c \end{cases} \tag{8}$$

The cutoff wavenumber κ_c is fixed by requiring that the rms height ζ of the small-scale spectrum equals $(4k)^{-1}$, where k denotes the radiation wavenumber. Wentz [1975] showed that variations in the perturbation parameter $k\zeta$ from 0.125 to 0.25 only slightly affects the T_B computations. Once κ_c is found the slope variance σ^2 of the large-scale spectrum is calculated by integrating $\kappa^2 S_\ell(\kappa)$ from $\kappa = 0$ to $\kappa = \kappa_c$. Table 3 gives the values of κ_c and σ^2 for the three frequencies.

Table 3. Cutoff Wavenumber and Large-Scale Slope Variance

Frequency	Cutoff Wavenumber κ_c	Large-Scale Slope Variance σ^2
1.4 GHz	2.4×10^{-2} cm^{-1}	1.3×10^{-4}
4.0 GHz	3.6×10^{-1} cm^{-1}	1.1×10^{-2}
7.5 GHz	7.7×10^{-1} cm^{-1}	2.7×10^{-2}

Downward Sky Brightness Temperature

The following expressions for the downward sky T_B angular distribution $T_s(\theta_z)$ are used in the model:

$$T_s(\theta_z) = (1-\tau)T_{eff} + \tau T_{cos} \tag{9}$$

$$\tau = (1 - T_{zen}/T_{eff})^{A(\theta_z)} \tag{10}$$

$$T_{eff} = 1.12\ T_{air} - 50 \tag{11}$$

where T_{air} is the air temperature given in Table 1, T_{zen} is the zenith atmospheric T_B, T_{cos} is the cosmic T_B, and $A(\theta_z)$ is the air mass function [Allen, 1963]. The above equations are the same as given by Peake [1969] except that the exponent $A(\theta_z)$ is used in place of sec θ_z.

Clear skies prevailed during the radiometer measurements, and Porter and Wentz's [1971] values for T_{zen} for a standard mid-latitude clear sky model are used and are given in Table 4. The cosmic T_B is the sum of the galactic T_B and the 2.7°K residual T_B of the primeval fireball. The spatial variation of the galactic T_B is quite large. Excluding discrete sources, the galactic center is about 35 times as bright as the cold sky for the frequencies being considered [Allen, 1963]. The cold sky is assumed, and the values for the galactic T_B and the cosmic T_B are shown in Table 4. Table 5 gives $T_s(\theta_z)$ for the three frequencies and for the rough-surface case. The smooth-surface values are essentially the same because the 3 K° difference in air temperature between the two environmental cases results in a change in $T_s(\theta_z)$ of only a few tenths of a K°.

Table 4. Input Parameters for the Sky Brightness Temperature Model

Frequency	Zenith Atmospheric T_B	Galactic T_B	Cosmic T_B
1.4 GHz	2.2°K	0.5°K	3.2°K
4.0 GHz	2.5°K	0.0°K	2.7°K
7.5 GHz	2.9°K	0.0°K	2.7°K

Table 5. Downward Sky Brightness Temperature Angular Distribution

Zenith Angle θ_z deg	$T_s(\theta_z)$ - °K 1.4 GHz	4.0 GHz	7.5 GHz
0	5.4	5.2	5.6
5	5.4	5.2	5.6
10	5.4	5.2	5.6
15	5.5	5.3	5.7
20	5.5	5.3	5.8
25	5.6	5.4	5.9
30	5.7	5.6	6.0
35	5.9	5.7	6.2
40	6.0	5.9	6.4
45	6.3	6.2	6.7
50	6.6	6.5	7.2
55	7.0	7.0	7.7
60	7.5	7.6	8.4
65	8.3	8.5	9.4
70	9.5	9.8	11.0
75	11.4	12.0	13.5
80	15.2	16.3	18.4
85	25.1	27.5	31.2
90	74.4	82.1	92.4

Correction for Antenna Patterns

The radiometer measurements reported by Swift [1974] are antenna temperatures T_A; that is, they are convolutions of T_B and the antenna gain patterns. Recent calculations by Beck [1975] show that the averaging effect of the antenna pattern produces significant differences between T_A and T_B. These differences, $\Delta T = T_A - T_B$, for the smooth surface are given in Table 6. Calculations were not done for $\theta = 0°$ or $10°$, and ΔT is assumed zero for these angles.

Furthermore ΔT is assumed independent of the environmental parameters, and the values in Table 6 are also used in the rough-surface computations. The effect of the antenna patterns on T_B is accounted for by adding ΔT to the T_B model computations.

Table 6. Antenna Pattern Corrections

Horizontal Polarization

Viewing Angle θ deg	$T_A - T_B$ (°K) 1.4 GHz	4.0 GHz	7.5 GHz
20	1.0	1.0	1.0
30	1.0	1.0	1.0
40	0.5	0.5	1.0
50	1.0	1.0	0.5
60	2.0	2.0	1.5
70	3.5	2.5	3.5

Vertical Polarization

Viewing Angle θ deg	$T_A - T_B$ (°K) 1.4 GHz	4.0 GHz	7.5 GHz
20	1.0	0.5	0.5
30	1.5	0.5	1.0
40	2.0	0.5	2.0
50	1.5	0.0	0.0
60	0.0	-2.5	-2.5
70	-9.0	-8.0	-14.0

Results

The model computations are compared with the measurements in Figures 1-3. The results for the three frequencies and for both polarizations are plotted versus viewing angle. The dashed and solid curves are the smooth-surface and rough-surface computations, respectively, and the squares and circles are the radiometer measurements of the smooth and rough surfaces, respectively. In general the agreement is good especially on the change in T_A produced by the

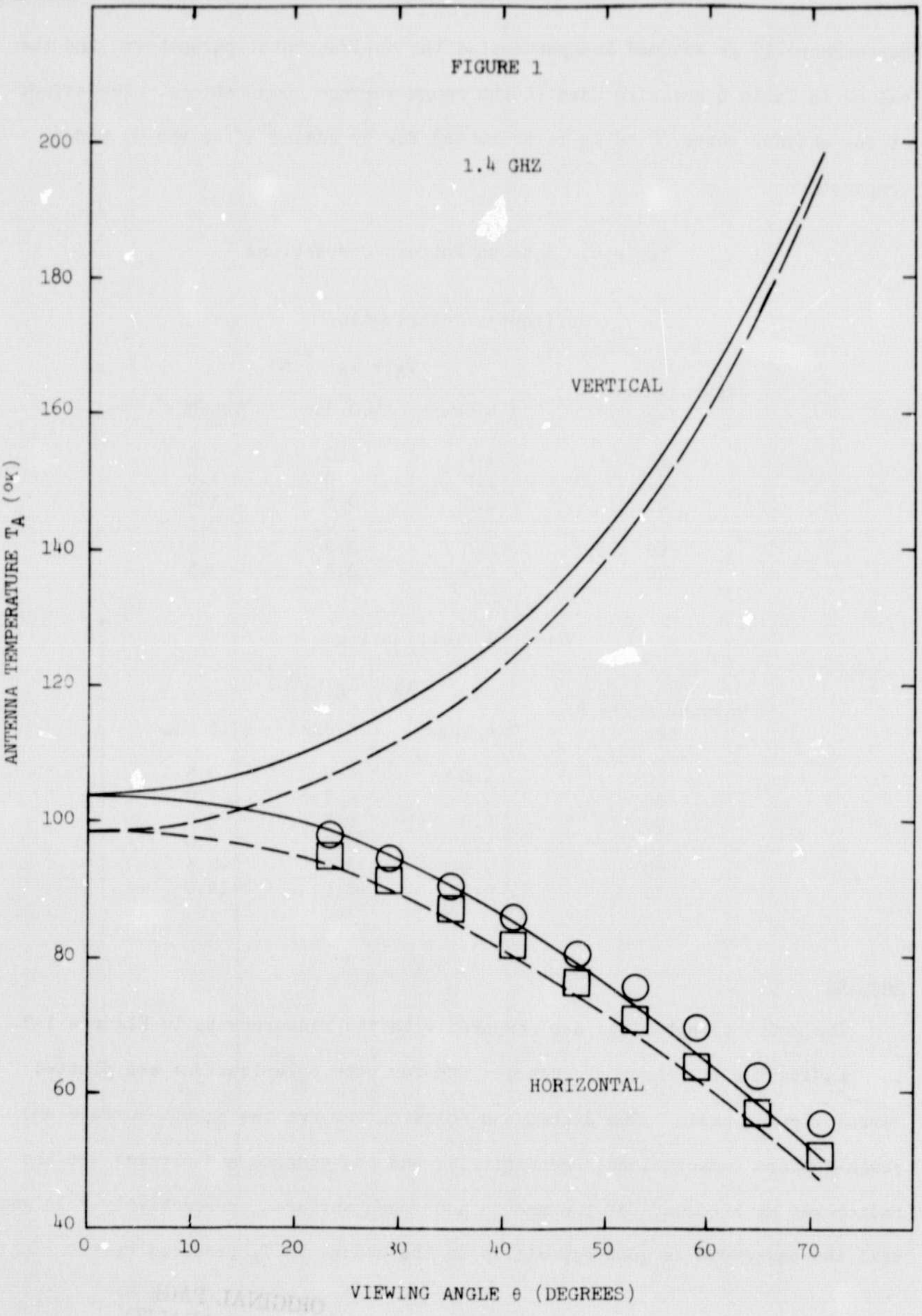

ORIGINAL PAGE IS OF POOR QUALITY

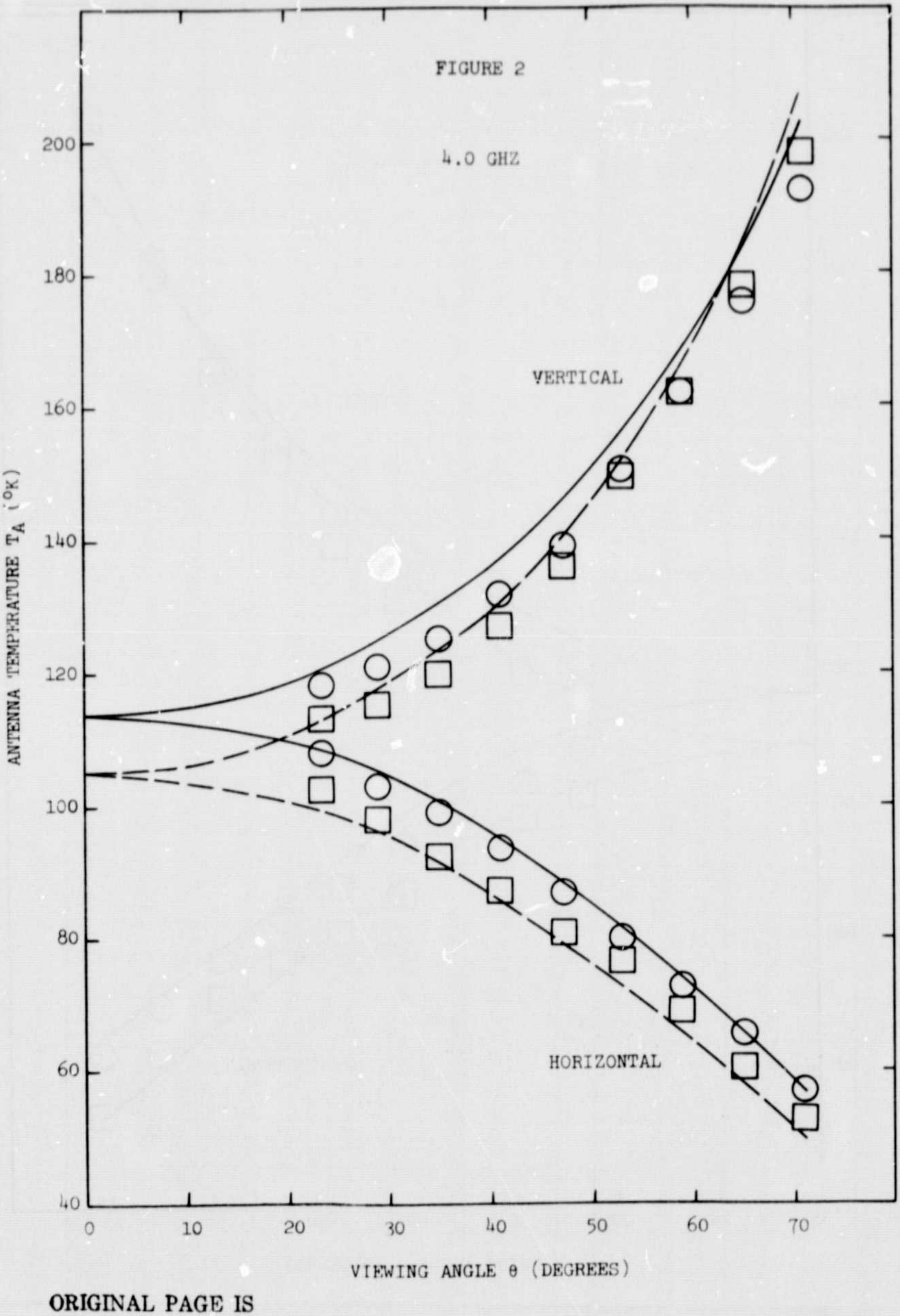

ORIGINAL PAGE IS OF POOR QUALITY

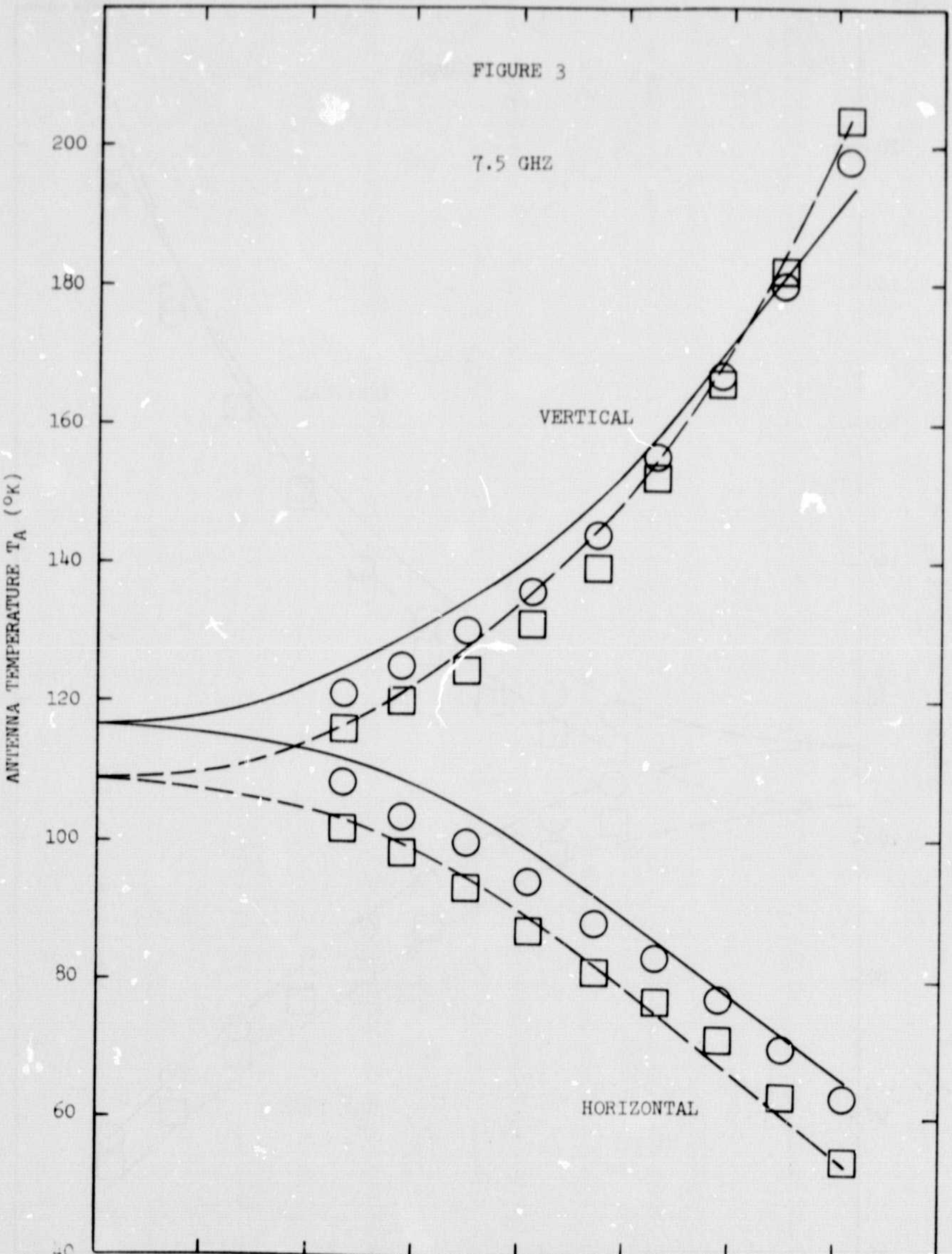
FIGURE 3
7.5 GHZ
VERTICAL
HORIZONTAL
ANTENNA TEMPERATURE T_A (°K)
VIEWING ANGLE θ (DEGREES)
40
60
80
100
120
140
160
180
200
0
10
20
30
40
50
60
70

presence of roughness. Discrepancies in magnitude do exist, but these are mostly less than twice the ± 2 K° error that is indicated by the size of the squares and circles. The agreement for horizontal polarization is somewhat better than for vertical polarization for which the computed T_A is greater than the measured T_A at intermediate viewing angles. The crossover of the smooth-surface and rough-surface curves for vertical polarization is in excellent agreement with the measurements at 7.5 GHz and in fair agreement at 4.0 GHz. No crossover occurs for the 1.4 GHz computations because essentially no large-scale roughness is present at this frequency as is indicated in Table 3.

Possible candidates contributing to the disagreements are listed below:

1. Error in specifying the power spectrum of the canal surface
2. Error in specifying the permittivity of the canal water, particularly at 1.4 GHz for which the permittivity is a strong function of the water temperature and salinity
3. Neglect of the large spatial variation of the galactic radiation at 1.4 GHz
4. Failure of the sky T_B model to consider atmospheric non-uniformities such as scattered clouds
5. Neglect of the contribution of the canal's shore to T_A
6. Failure to use the total antenna pattern in computing T_A
7. Neglect of intermediate-scale roughness by the two-scale scattering model
8. Experimental calibration error

References

Allen, C. W., Astrophysical Quantities, pp. 120-126, Oxford University Press, New York, 1963.

Beck, F. B., Antenna pattern corrections to microwave radiometer temperature calculations, Radio Science, Oct. 1975.

Cardone, V. J., Specification of the wind field distribution in the marine boundary layer for wave forecasting, Rep. TR 69-1, Geophys. Sci. Lab., New York Univ., New York, Dec. 1969.

Ho, W. W., and W. F. Hall, Measurements of the dielectric properties of seawater and NaCl solutions at 2.65 GHz, J. Geophys. Res., 78(27), 6301-6315, 1973.

Hollinger, J. P., Passive microwave measurements of sea surface roughness, IEEE Trans. Geosci. Electron., 9(3), 165-169, 1971.

Peake, W. H., The microwave radiometer as a remote sensing instrument, Tech. Rep. 1903-8, NASA Grant NSR-36-008-027, The Ohio State University, Columbus, Ohio, 1969.

Pierson, W. J., and R. A. Stacy, The elevation, slope, and curvature spectra of a wind roughened sea surface, Contract. Rep. NASA CR-2247, Langley Res Center, NASA, Hampton, VA, Dec. 1973.

Porter, R. A., and F. J. Wentz, Microwave radiometric study of ocean surface characteristics, Contract. Rep. 135140, Nat. Environ. Satell. Serv., NOAA, Washington, D. C., July 1971.

Swift, C. T., Microwave radiometer measurements of the Cape Cod Canal, Radio Science, 9(7), 641-653, 1974.

Wentz, F. J., A two-scale scattering model for foam-free sea microwave brightness temperatures, J. Geophys. Res., 80(24), 1975.

1. Report No.
NASA CR-145277

2. Government Accession No.

3. Recipient's Catalog No.

4. Title and Subtitle
Computation of Theoretical Brightness Temperatures Corresponding to the Cape Cod Canal Radiometer Measurements

5. Report Date
November 1977

6. Performing Organization Code

7. Author(s)
Frank J. Wentz

8. Performing Organization Report No.
Part I

10. Work Unit No.

9. Performing Organization Name and Address
Frank J. Wentz and Associates
Box 162, MIT Branch P.O.
Cambridge, MA 02139

11. Contract or Grant No.
L-24420A

12. Sponsoring Agency Name and Address
National Aeronautics and Space Administration
Washington, D. C. 20546

13. Type of Report and Period Covered
Final Report

14. Sponsoring Agency Code

15. Supplementary Notes

16. Abstract

Theoretical brightness temperatures are computed from the ground-truth data that was collected during the radiometer measurements of the Cape Cod Canal. An approximate correction for antenna pattern effects is made, and the results are compared with the radiometer measurements.

17. Key Words (Suggested by Author(s))
Microwave radiometer
Antenna temperature
Brightness temperature

18. Distribution Statement
Unclassified
Unlimited Subject Category 48

19. Security Classif. (of this report)	20. Security Classif. (of this page)	21. No. of Pages	22. Price*
Unclassified	Unclassified	12	$4.00

* For sale by the National Technical Information Service, Springfield, Virginia 22161